

Critical Fluctuations in Membranes

Ruitian Zhang,¹ Wenjun Sun,¹ Stephanie Tristram-Nagle,² R. L. Headrick,³ Robert M. Suter,¹ and John F. Nagle^{1,2}

¹Department of Physics, Carnegie Mellon University, Pittsburgh, Pennsylvania 15213

²Department of Biological Sciences, Carnegie Mellon University, Pittsburgh, Pennsylvania 15213

³Cornell High Energy Synchrotron Source, Ithaca, New York 14853

(Received 28 October 1994)

High resolution x-ray scattering measurements on model membranes consisting of fully hydrated lipid bilayers have been performed to evaluate the origin of the anomalous temperature dependence of the lamellar D spacing. The data are well fit by our recent refinement of the theory of power law tails that occur in fluctuating smectic liquid crystals. The data show that the anomalous increase in D is due to an increase in the thickness of the bilayer, caused by critical straightening of the hydrocarbon chains, and that little change in undulation force takes place.

PACS numbers: 87.22.Bt, 05.70.Jk, 64.70.Md, 87.64.Bx

Fluctuations are vital in biological systems [1]. As is well known in condensed matter physics [2], fluctuations are enhanced when a critical point is approached by varying thermodynamic parameters such as temperature or composition. Biomembranes, in particular, undergo phase transitions, and it appears that the main hydrocarbon chain melting transition in the lipid bilayer component occurs in the vicinity of a critical point [3–6]. Analogous to other liquid crystal transitions that exhibit pretransitional critical behavior [7], this one exhibits the buildup of fluctuations that would lead to a critical point if not preempted by a first order transition.

One physical quantity that shows anomalous temperature dependence is the lamellar D spacing in samples of lipid bilayers that are lyotropic smectic liquid crystals. Locally, the bilayers are extended in the x - y plane and stacked along the z axis with a mean repeat spacing D , which consists of the sum of the thickness of the lipid bilayer D_B plus the water space D_W between bilayers. The D spacing is easily measured from the lamellar (00 h) x-ray scattering peaks; the thicknesses D_B and D_W are not directly measurable, and have only been deduced from interpretation fraught with difficulties [8]. In agreement with previous measurements [9–14] our data in Fig. 1 show that D increases with increasing rapidity as T is decreased to the main transition temperature T_M near 24°C. Such thermal behavior is characteristic of critical fluctuations.

One interpretation of the anomalous $D(T)$ behavior [12], which will be called model I, attributes the increase in D to an increase in D_W . The proposed physical mechanism for model I is increased undulation fluctuations in the bilayers brought about by a reduced curvature modulus K ; the reduced curvature modulus is supposed to be due to increased density fluctuations in the plane of each monolayer in the bilayer. A reduced K would increase the Helfrich [15] repulsive force between the bilayers in the multilamellar vesicle and thereby increase D_W . This plausible scenario might, however, not necessarily be relevant,

because the unknown magnitude of the phenomenological parameter that couples density fluctuations to K could be too small to have much effect.

An alternative interpretation for the increase in D , which we will call model II, is that it is due primarily to an increase in bilayer thickness D_B . It is generally agreed that the chain melting transition involves a change in the conformations of the hydrocarbon chains into straighter, more extended forms; the 2 Å increase in chain length required for the 4 Å increase in D_B is safely smaller than the increase (at least 4 Å/chain) in going to phases with nearly complete chain ordering [3,8]. Like the first interpretation, model II also supposes that the main transition has critical character so that the chain extension and the thickening of D_B accelerate as the transition is approached from higher temperatures. It has been suggested [4] that the critical character of this transition could be similar to the simplest kinds of striped commensurate-incommensurate transitions; this theory, when extended to three dimensions, predicts that $dD(T)/dT$ should diverge as $\ln(T - T_c)$ near T_c [16]. It is not possible, however, to confirm or disprove this

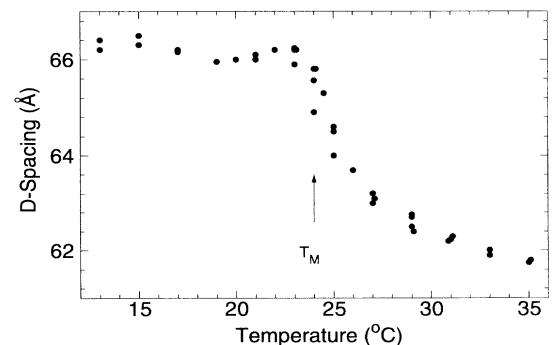


FIG. 1. Temperature dependence of the D spacing of fully hydrated, unoriented bilayer dispersions of DMPC. The transition from the high temperature chain melted phase to the lower temperature ripple phase occurs at T_M .

functional form from the data in Fig. 1, because the asymptotic region cannot be accessed due to intercession of the first order transition.

This Letter reports an x-ray scattering experiment that discriminates between models I and II. The detailed line shapes of the lamellar (00*h*) scattering peaks reveal interbilayer fluctuations that include both undulations and compression [17,18]. The most important parameter in the theory of scattering due to these fluctuations is Caillé's $\eta = (kTq^2/8\pi)(BK)^{-1/2}$, where B is the compression modulus for stacks of bilayers. Large values of η yield large scattering tails that behave asymptotically as $|q - q_h|^{-1+\eta}$ for powder samples [19]. The solid curves in Fig. 2 show the theoretical shapes of these peaks [20].

According to model I, as T approaches T_M , K decreases and D_W increases. Also, the compression modulus B must decrease. Let us estimate the effect upon scattering, i.e., the increase in η , by considering the forces between bilayers. The van der Waals energy is given by

$$E_W = -\frac{W}{12\pi} \left(\frac{1}{D_W^2} - \frac{2}{(D_W + D_B)^2} + \frac{1}{(D_W + 2D_B)^2} \right), \quad (1)$$

where W is about 5×10^{-14} erg [21]. The energy of the phenomenological hydration force is usually given as

$$E_H = P_h \Lambda e^{-D_W/\Lambda}. \quad (2)$$

For the undulation (free) energy Helfrich gave

$$F_{U1} = \frac{3\pi^2}{128} \frac{(kT)^2}{\kappa D_W^2}, \quad (3)$$

where $\kappa = KD$ is the bending rigidity which has been measured to be about 10^{-12} erg [22]. It has been argued

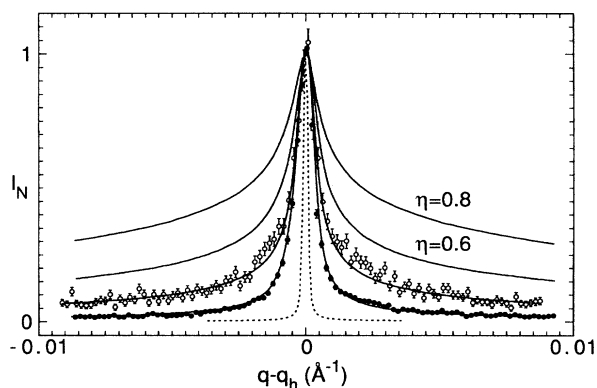


FIG. 2. Normalized theoretical scattering intensities are shown by solid curves for $\eta = 0.19, 0.41, 0.6,$ and 0.8 , proceeding from bottom to top. Normalized scattering intensity data for the first 2 orders of DMPC at 24.3°C are shown by filled circles for the $h = 1$ peak and open circles for the $h = 2$; the simultaneous theoretical fit ($\chi^2 = 1.46$) is shown by the two lower solid curves. The in-plane resolution is shown by the dotted curve.

that compressional forces should modify this energy, and the following form has been offered [23,24]:

$$F_{U2} = (\pi kT/16) (P_h/\kappa\Lambda)^{1/2} e^{-D_W/2\Lambda}. \quad (4)$$

Although there are small differences in the values of the parameters depending upon how the undulation force is treated, evaluations from osmotic pressure data for egg phosphatidylcholine bilayers above T_M give $P_h = 5 \times 10^8$ erg/cm³ and $\Lambda = 1.4-1.7$ Å [25]. If D_W increases by 3 Å as T approaches T_M , as required by model I and the data in Fig. 1, minimization of the total energy shows that K must decrease by a factor of 0.48 if Eq. (3) is used and by a factor of 0.21 if Eq. (4) is used. Also, the compressional modulus B , which is the curvature in the total free energy at the bottom of the well, decreases by a factor of 0.17 if Eq. (3) is used and by 0.81 if Eq. (4) is used. From these estimates we conclude that model I requires that η should increase by at least a factor of 2 as T approaches T_M .

High resolution x-ray scattering data were obtained at CHESS on the F3 station. A double bounce Si monochromator was tuned to 1.2147 Å x rays, the scattering angles were selected by a Si analyzer crystal, and the intensity was measured by a scintillation detector. In-plane resolution was measured to be 2×10^{-4} Å⁻¹ FWHM and out-of-plane resolution was estimated geometrically to be 0.012 Å⁻¹. Sample exposure times were limited to 10 min even though there was no detectable change in peak shapes up to 30 min. The samples, contained in 1.5 mm glass capillaries, were 70% water/30% DMPC (dimyristoylphosphatidylcholine), which was obtained from Avanti Lipids (Alabaster, AL).

Figure 2 shows the first and second order lamellar peaks for DMPC at a temperature only slightly above the main transition temperature, $T_M = 24.0^\circ\text{C}$ [26]. The peaks in Fig. 2 clearly have long tails due to interbilayer fluctuations; the background measured from the capillary filled only with water was less than half the lipid bilayer scattering even at the ends of the q range shown, and this nearly constant background has been subtracted. Another signature of interbilayer fluctuations is the relatively larger tails for the $h = 2$ peak than for the $h = 1$; this is expected because the η parameter theoretically scales as h^2 for higher order peaks [17].

The two lower solid curves in Fig. 2 show the theoretical fit to the data using Eq. (80) in [20]. The goodness of the fit confirms that the data reflect interbilayer fluctuations. The fit yields values for the peak positions, from which D is calculated using Bragg's law, and the peak heights. The fits yield a mean coherence length $L = 4800$ Å, a distribution $\sigma_L = 4200$ Å in L , and an out-of-plane resolution 0.013 Å⁻¹, all of which have been constrained to be the same for both the $h = 1$ and 2 peaks. Most importantly, the fit yields the Caillé parameters $\eta_1 = 0.19$ and $\eta_2 = 0.41$. We have consistently

obtained $\eta_2 < 4\eta_1$ and feel that this may be associated with deviations from the harmonic approximation [17], but this should not detract from the overall success of the theory.

The scattering peaks for data taken at higher temperatures yield a considerably smaller D as shown in Fig. 1. Figure 3 compares the shape of the $h = 2$ peak taken at 33°C with the $h = 2$ peak at 24.3°C. This comparison shows that the tails at the higher temperature and smaller D are essentially the same as when the sample is near T_M . The $h = 1$ tails at the two temperatures (not shown) are also nearly the same. In confirmation of this visual impression, the results for the η 's at 33°C are nearly the same as at 24.3°C, despite the difference of 3.6 Å in D . This result is inconsistent with model I.

Another important discriminator between models I and II is the relative intensities $I(h)$ of the different lamellar peaks ($00h$). In model I the bilayer thickness D_B is supposed to not change much, so the discrete bilayer form factors $F(q_h)$ derived from $I(h)$ should lie on the same continuous transform $F(q)$, defined as

$$F(q) = \int_{-D/2}^{D/2} \rho(z) e^{iqz} dz, \quad (5)$$

where $\rho(z)$ is the electron density in the direction perpendicular to the bilayers minus the electron density of the aqueous solvent [27]. In model II, however, the bilayer thickness D_B changes, so $\rho(z)$ changes and the form factors at different temperatures should not lie on the same $F(q)$ transform. Examples of continuous transforms are shown in Fig. 4. The general character of the transform for lecithin bilayers for $q < 0.3 \text{ \AA}^{-1}$ is well established from many studies [25]; the first two discrete form factors

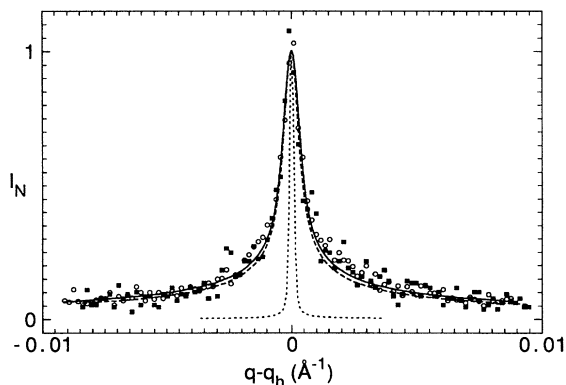


FIG. 3. Normalized scattering intensity data for the $h = 2$ peak for DMPC at 24.3°C (open circles) and at 33°C (filled squares). The dotted line shows the in-plane resolution. The solid line shows the same fit to the data at 24.3°C as in Fig. 2. The dashed line shows the fit to the data at 33°C with $\eta_1 = 0.16$, $\eta_2 = 0.40$, $L = 6000 \text{ \AA}$, $\sigma_L = 3800 \text{ \AA}$, and $\chi^2 = 1.37$. Constraining L and σ_L to the same values obtained in Fig. 2 did not change the η values significantly and χ^2 only increased to 1.38.

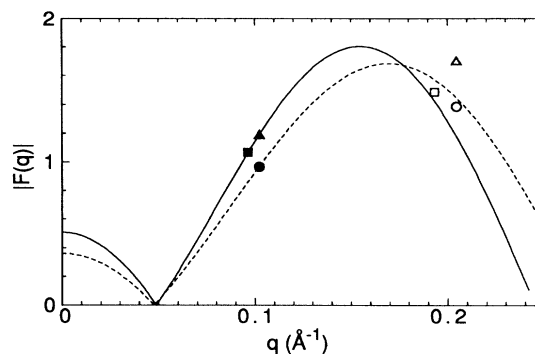


FIG. 4. Two continuous transforms $F(q)$ for a simple model with $D_B = 37.2 \text{ \AA}$ (solid curve) and $D_B = 33.6 \text{ \AA}$ (dashed curve). The symbols show form factors $F(q_h)$, the squares are for $T = 24.3^\circ\text{C}$, the circles are for $T = 33^\circ\text{C}$, the filled symbols are for $h = 1$, and the open symbols are for $h = 2$. The triangles also show the form factors for $T = 33^\circ\text{C}$, but scaled so that $F(q_1)$ falls on the solid curve.

$F(2\pi/D)$ and $F(4\pi/D)$ have the same negative sign and comparable magnitudes. The particular transforms shown in Fig. 4 for different bilayer thicknesses D_B are for a simple electron density model consisting of delta functions at $|z| = \pm D_B/2$ representing the headgroups, a uniform electron density ρ_{HC} in the hydrocarbon interior of the bilayer, $|z| < D_B/2$, and a zero (relative to water) electron density elsewhere. Volume measurements [26] and a fundamental relation for $F(0)$ [28] constrain the number of parameters in this simple model to one, which may be taken to be D_B . More realistic models increasingly affect the transforms at higher q values, but this simple model should be a good guide for the first 2 orders.

To obtain the form factors $F(q_h)$ from the measured intensities when the scattering peaks are affected by interbilayer fluctuations is nontrivial. In particular, naive integration of the central scattering peaks gives incorrect answers because it does not account for the considerable scattering spread out in the long tails that cannot be measured accurately because of background and because the form factors depend upon q . However, the detailed fitting to the accurately measured data shown in Figs. 2 and 3 also allows one to obtain the magnitudes of the discrete form factors $|F(2\pi h/D)|$ [20].

By measuring the scattering at the first and second order peaks for the same sample we obtained the ratios $R_{21} = |F(4\pi/D)/F(2\pi/D)|$. For 33°C R_{21} is 1.43 and R_{21} decreases to 1.39 at 24.3°C. These ratios are inconsistent with any reasonable continuous transform, such as those shown in Fig. 4, because, when D increases upon going from 33 to 24°C, $|F(2\pi/D)|$ should decrease and $|F(4\pi/D)|$ should increase, thereby increasing R_{21} rather than decreasing it. This is inconsistent with model I.

We therefore considered model II which requires a different transform at each temperature such as the two shown in Fig. 4. Although our data did not yield accurate

ratios of the form factors for two different temperatures, our data are consistent (within 5%) with placing the two first order form factors on the continuous transforms with the corresponding bilayer thicknesses D_B used in Fig. 4. Then, our measured ratios R_{21} require the values of the second order form factors shown in Fig. 4; the agreement with the continuous transforms $F(q)$ is adequate in view of the simple electron density model employed. This result is consistent with model II. The triangles in Fig. 4 again demonstrate that model I is inconsistent since all four form factors cannot be put on the same continuous transform.

In conclusion, high resolution x-ray scattering and detailed peak shape analysis show that DMPC bilayers thicken critically as the main transition temperature T_M is approached from higher temperatures. The biological relevance of this result is that bilayer thickness would be sensitively tunable thermodynamically; this could modulate the accommodation of proteins and their functionality [29,30].

This research was supported by NIH Grant GM-44976 (CMU) and NSF Grant DMR-9311772 (CHESS).

-
- [1] H. Frauenfelder, in *Biological Physics*, edited by E.V. Mielczarek *et al.* (AIP, New York, 1993).
- [2] M.E. Fisher, *Rep. Prog. Phys.* **30**, 615 (1967).
- [3] J.F. Nagle, *Annu. Rev. Phys. Chem.* **31**, 157 (1980).
- [4] J.F. Nagle, C.S.O. Yokoi, and S.M. Bhattacharjee, in *Phase Transitions*, edited by C. Domb *et al.* (Academic Press, New York, 1989), Vol. 13, p. 235.
- [5] A. Ruggiero and B. Hudson, *Biophys. J.* **55**, 1111 (1989).
- [6] I. Hatta, K. Suzuki, and S. Imaizumi, *J. Phys. Soc. Jpn.* **52**, 2790 (1983).
- [7] T.W. Stinson and J.D. Litster, *Phys. Rev. Lett.* **30**, 688 (1973).
- [8] J.F. Nagle and M.C. Wiener, *Biochim. Biophys. Acta* **942**, 1 (1988).
- [9] Y. Inoko and T. Mitsui, *J. Phys. Soc. Jpn.* **44**, 1918 (1978).
- [10] M. Janiak, D.M. Small, and G.G. Shipley, *Biochemistry* **15**, 4575 (1976).
- [11] S. Matuoka, S. Kato, and I. Hatta, *Biophys. J.* **67**, 728 (1994).
- [12] T. Hønger, K. Mortensen, J.H. Ipsen, J. Lemmich, R. Bauer, and O.G. Mouritsen, *Phys. Rev. Lett.* **72**, 3911 (1994).
- [13] G.S. Smith, E.B. Sirota, C.R. Safinya, R.J. Plano, and N.A. Clark, *J. Chem. Phys.* **92**, 4519 (1990).
- [14] S. Kirchner and G. Cevc, *Europhys. Lett.* **23**, 229 (1993).
- [15] W. Helfrich, *Z. Naturforsch.* **33a**, 305 (1978).
- [16] S.M. Bhattacharjee, J.F. Nagle, D.A. Huse, and M.E. Fisher, *J. Stat. Phys.* **32**, 361 (1983).
- [17] A. Caillé, *C. R. Acad. Sci. Ser. B* **274**, 891 (1972).
- [18] J. Als-Nielsen, J.D. Litster, R.J. Birgeneau, M. Kaplan, C.R. Safinya, A. Lindegaard-Anderson, and S. Mathiesen, *Phys. Rev. B* **22**, 312 (1980).
- [19] D. Roux and C.R. Safinya, *J. Phys. (Paris)* **49**, 307 (1988).
- [20] R. Zhang, R.M. Suter, and J.F. Nagle, *Phys. Rev. E* **50**, 5047 (1994).
- [21] J.N. Israelachvili, *Intermolecular and Surface Forces* (Academic Press, London, 1985), p. 149.
- [22] M.B. Schneider, J.T. Jenkins, and W.W. Webb, *Biophys. J.* **45**, 891 (1984).
- [23] E. Evans and D. Needham, *J. Phys. Chem.* **91**, 4219 (1987).
- [24] R. Podgornik and V.A. Parsegian, *Langmuir* **8**, 557 (1992).
- [25] T.J. McIntosh, A.D. Magid, and S.A. Simon, *Biochemistry* **26**, 7325 (1987). Note that the given value of P_h uses a different definition of fluid spacing, about 12 Å smaller than our D_w .
- [26] J.F. Nagle and D.A. Wilkinson, *Biophys. J.* **23**, 159 (1978).
- [27] C.R. Worthington, G.I. King, and T.J. McIntosh, *Biophys. J.* **13**, 480 (1974).
- [28] J.F. Nagle and M.C. Wiener, *Biophys. J.* **55**, 309 (1989).
- [29] S.M. Gruner and E. Shyamsunder, *Ann. N.Y. Acad. Sci.* **625**, 685 (1991).
- [30] M. Bloom, E. Evans, and O.G. Mouritsen, *Q. Rev. Biophys.* **24**, 293 (1991).